https://doi.org/10.2352/ISSN.2470-1173.2019.4.PMII-578

Face Skin Tone Adaptive Automatic Exposure Control

Noha El-Yamany, Jarno Nikkanen (Intel Corporation; Tampere, Finland) and Jihyeon Yi (Intel Corporation; Seoul; Korea)

Abstract

In face-priority automatic exposure control in digital camera systems, exposure adjustment is typically made irrespective of the face skin tone, i.e. how dark or bright the face is. As a result, a face can become over exposed when it is present against a very dark background, or become under exposed when it is present against a very bright background, depending on the face skin tone and scene content. Adapting the exposure control to the face skin tone will result in well-exposed faces in various capture scenarios, and hence better image quality.

This paper presents a novel face skin tone adaptive automatic exposure control solution. Using a well-trained neural network based face skin tone predictor, the likelihoods of dark and bright face skin tones are calculated. An algorithm adjusts the bounds of the target brightness of the exposure control based on the face skin tone likelihoods and a set of configuration parameters. The face skin tone adaptive brightness bounds then guide the frame exposure adjustment. Experimental results demonstrate the outperformance of the proposed solution over conventional exposure control that does not take into account the face skin tone information.

Introduction

Digital cameras are widely used and are present in everyday products, such as smart phones, tablets, phablets, notebooks, cars and wearable computing systems, just to name a few examples. Exposure control [1-12] is an essential camera control algorithm (CCA) in digital cameras. It plays a crucial role in adjusting the brightness of the photographed scene, while preserving its information content, within the camera sensor constraints, such as the sensor sensitivity, noise characteristics and dynamic range. Correct exposure is also crucial for the proper operation of other CCAs, such as white balancing and focusing algorithms. Two typical examples of information loss due to improper exposure control are *underexposure*, which results in quantization of pixels to very small values or zero, and *overexposure*, which results in saturation of pixels. The goal of exposure control is to render well-exposed scenes with as minimal information loss as possible.

In many capture scenarios and camera uses cases, there are persons in the scene, and their faces are of higher priority than everything else being photographed. It is not a surprise, therefore, that nowadays there are face-priority features available in many digital camera systems. In the context of exposure control, face priority guides the scene brightness adjustment such that the face, which has the higher priority, is exposed well with minimal information loss. Typically, in face-priority exposure control, the adjustment of the exposure time and other exposure parameters is made irrespective of the face skin tone; i.e. how dark or bright the face is. As a result, a face with a dark skin tone can become over exposed when it is present against a very dark background, or a face with a bright skin tone can become under exposed when it is present against a very bright background. Adapting the exposure control to the face and its skin tone [13] will result in well-exposed faces in various capture scenarios, and hence better image quality and end-user satisfaction. To the best of our knowledge, there is no published work on face skin tone adaptive exposure control. One relevant work is in [13], which addresses the concept of using the face skin tone information in brightness and color adjustment in a digital camera system.

In this paper, a novel face skin tone adaptive automatic exposure control (FaSTA AEC) solution is presented. A neural network based face skin tone predictor (FSTP) is designed and trained to produce reliable likelihoods for the dark and bright face skin tones for the detected face in the input frame. The bounds of the target brightness of the exposure control are then adjusted based on the face skin tone likelihoods and a set of configuration parameters. The face skin tone adaptive brightness bounds then guide the frame exposure adjustment, to render well-exposed faces.

The rest of the paper is organized as follows. First, an overview of the proposed solution is given, followed by detailed description of the FSTP, and the conventional and FaSTA AEC brightness adjustments. Example results are then demonstrated and discussed for two challenging capture scenarios. Finally, conclusions and future work items are provided.

Overview of the Proposed Solution

Figure 1 depicts a schematic diagram of the FaSTA AEC solution. Face detection is performed on the luma component (***I***) of the frame output from the camera image processing pipeline, in order to locate the face region in the frame. Eye detection is then performed in the face region in order to find the positions of both of the left and right eyes. Given ***I*** and both of the eye positions, the face image is aligned, and face skin tone prediction is performed on the aligned face, in order to calculate the corresponding face skin tone likelihood. An algorithm then calculates the bounds on the exposure control target brightness based on the face skin tone likelihoods and a set of configuration (tunable) parameters. The calculated face skin tone adaptive brightness bounds are then used to guide the calculation of the exposure parameters.

Face Skin Tone Prediction

The function of the FSTP is to predict the face skin tone, providing the face bright and dark skin tone likelihoods. The FSTP algorithm pipeline is depicted in Figure 2. Given the positions of the left and right eyes, which are used as facial landmarks, the input face image

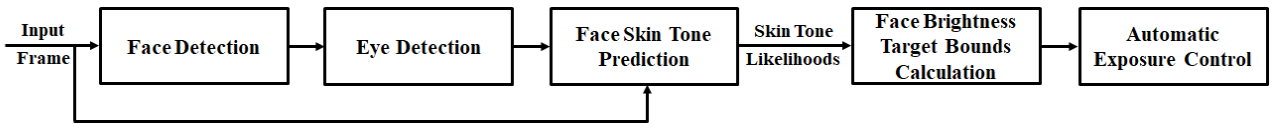

Figure 1 Schematic Diagram of the Face Skin Tone Adaptive Automatic Exposure Control Solution

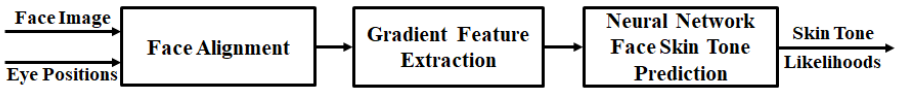

Figure 2 Schematic Diagram of the Face Skin Tone Predictor

is aligned to a template of pre-defined image size and eye positions. A gradient feature vector is calculated from the aligned face image. The gradient feature vector is then fed to a pre-trained neural network (NN) predictor, whose output is the face dark and bright skin tone likelihoods.

A. Face Alignment

As noted earlier, let $\boldsymbol{I}$ denote the luma component of the input frame to face detection, and in which there is a face present. Let $\boldsymbol{E}_{left}(x,y)$ and $\boldsymbol{E}_{right}(x,y)$ denote the locations of the left and right eyes, respectively, in the detected face in $\boldsymbol{I}$. x and y refer to the x-coordinate and y-coordinate, respectively. Using $\boldsymbol{E}_{left}$ and $\boldsymbol{E}_{right}$, the facial image is aligned to have a pre-defined size of 48×48 and eye positions of (12,12) and (35,12) for the left and right eyes, respectively, as depicted in Figure 3.

The alignment is performed via a 2×3 similarity transformation [14] calculated based on the eye positions in $\boldsymbol{I}$ and the pre-defined eye positions in the aligned image template. 5×5 Gaussian filtering (with $\sigma = 1$) is used for pixel interpolation. The pre-defined size of the aligned face image, $\boldsymbol{I}_{aligned}$, and the pre-defined values of the eye positions in $\boldsymbol{I}_{aligned}$ are selected based on experimentation. It is worth mentioning that the computational cost of face skin tone prediction will increase as the size of the aligned face image increases. Face alignment helps to obtain a similar face image regardless of the scale and face roll angle. One should note, however, that if the face in $\boldsymbol{I}$ has large pitch or yaw angle, the alignment may not render the desired result. This limitation will be addressed in future work.

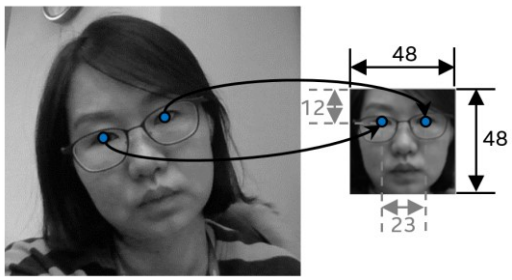

Figure 3 Illustration of Facial Image Alignment

B. Gradient Feature Extraction

Given $\boldsymbol{I}_{aligned}$, an integral image [15] is calculated, in order to boost the speed of the following step of feature extraction [16]. The size of the integral image is the same as the size of the aligned face image, i.e. also 48×48. Given the integral image, a gradient feature vector is computed based on 16-dimensional U-SURF descriptors [16]. Figure 4 depicts the aligned image sampling points (i.e. the interest points) at which the U-SURF descriptors are calculated. The sampling step s and margin m are both set to 6. Padding of the 48×48 aligned image is performed to create the margin m. At each sampling point, a U-SURF descriptor is calculated for a patch (region) of 10×10 pixels. To calculate the U-SURF descriptor at a given sampling point (k,l), where $k = [1, 2,...,7]$ and $l = [1, 2,...,7]$, the corresponding 10×10 region is divided into 4 sub-regions, R_i, where $i = [1, 2, 3, 4]$, as shown in Figure 4. The sampling point is the top-left corner pixel in the sub-region R_1. For the 7×7 sampling grid, a total of 49 U-SURF descriptors are calculated. For sub-region i, the 4-dimensional U-SURF descriptor vector $\mathbf{v}_{k,l,i}$, is calculated as in [16]. The 4-dimensional U-SURF descriptor vector at sampling point (k,l) and for sub-region i, $\mathbf{v}_{k,l,i}$, is calculated as in [16]. Let d_x and d_y denote the horizontal and vertical Haar wavelet responses calculated for a given sub-region. $\mathbf{v}_{k,l,i}$ is defined as [16]

$$\mathbf{v}_{k,l,i} = (\Sigma d_x, \Sigma d_y, \Sigma|d_x|, \Sigma|d_y|) \quad (1)$$

The 16-dimensional U-SURF descriptor for each sampling point (k,l), $\mathbf{V}_{k,l}$, is calculated by concatenating the descriptor vectors $\mathbf{v}_{k,l,i}$ for the corresponding 4 sub-regions, i.e.

$$\mathbf{V}_{k,l} = Concatenate\,(\mathbf{v}_{k,l,1}, \mathbf{v}_{k,l,2}, \mathbf{v}_{k,l,3}, \mathbf{v}_{k,l,4}) \quad (2)$$

For $\boldsymbol{I}_{aligned}$, a total of 16-dimensional 49 descriptor vectors are calculated for the 49 sampling points. The concatenation of all of those 49 vectors forms the 784-dimensional gradient feature vector $\mathbf{G}$ for the aligned image

$$\mathbf{G} = Concatenate\,(\mathbf{V}_{k,l})\ \forall\ k,\ l \in [1,2,..7] \quad (3)$$

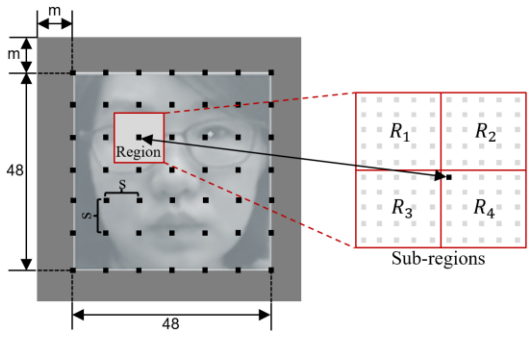

Figure 4 Sampling (Interest) Points, Region and Sub-regions for the U-SURF Descriptors

C. Neural Network Face Skin Tone Prediction

Face skin tone prediction is performed via a small-sized, pre-trained neural network. During inference, the input to the NN is the aligned facial image 784-dimensional gradient feature vector, $\mathbf{G}$, and the output is the 2-dimensional face skin tone likelihood vector $\boldsymbol{L} = [\boldsymbol{L}_{dark}, \boldsymbol{L}_{bright}]$, where $\boldsymbol{L}_{dark}$ and $\boldsymbol{L}_{bright}$ are the dark and bright face skin tone likelihoods, respectively, and both $\boldsymbol{L}_{dark}$ and $\boldsymbol{L}_{bright} \in [0.0, 1.0]$, and they sum to unity. The implicit assumption for using the gradient feature vector as input to the NN is that the relationship between the facial features correlate with the ethnicity, hence the skin tone. That assumption governed how the data sets used for training, validating and testing the NN were annotated. The gradient features are also robust over a relatively wide range of exposure.

The NN has a feed-forward, fully-connected architecture, with two hidden layers and one output layer. Each of the hidden layers has 200 neurons. The activation function of the hidden layers is chosen to be the leaky rectified linear unit ReLU [17, 18] with alpha

parameter = 0.1. The softmax function is used in the output layer. This simple NN architecture is chosen to keep the computational cost for the FSTP low. It is worth mentioning that a 784-dimensional mean vector is calculated over all the training data gradient feature vectors. That mean vector is subtracted from **G** and the result is normalized to a pre-defined range, before inputting it to the NN to calculate the face skin tone likelihoods.

During the network training phase, iterative stochastic gradient descent was pursued to find the optimal network weights. The network was trained using a subset of the MORPH data set [19, 20], which contains thousands of portrait face images for different ethnic groups, such as Africans, Europeans, Asians, Hispanics and others. The training, testing and validation data sets had equal number of dark and bright faces, as depicted in Table 1, in order to guarantee consistent skin tone prediction performance for both dark and bright faces. The annotation of the face skin tone for the training, testing and validation data sets was done both objectively (based on ethnicity) as well as subjectively.

Table 1: Composition of the FSTP Training, Validation and Testing Data Sets

Annotation	Training Set	Validation Set	Testing Set
Dark	~ 36K	~ 4K	~ 3.5K
Bright	~ 36K	~ 4K	~ 3.5K
Total	**~ 72K**	**~ 8K**	**~ 7K**

The receiver operating characteristic (ROC) curves for the FSTP for both dark and bright face skin tones are depicted in Figure 5. The curves were generated for ~ 14K test images (the ~ 7K test images and their mirrored ones, which are used as a form of data augmentation). The points that correspond to a skin tone likelihood threshold of 0.75 are shown on the curves as large dots. The FSTP trained NN model resulted in consistently high likelihood values for both dark and bright faces, as will be demonstrated later in the Experimental Results section.

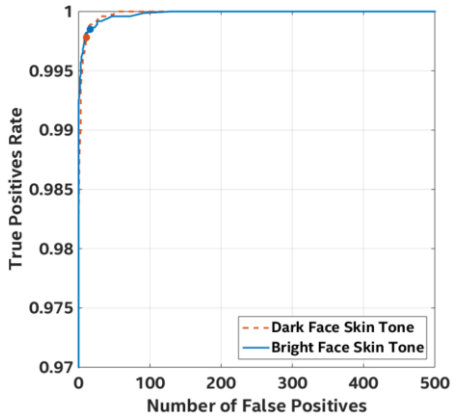

Figure 5 The ROC Curves of the Face Skin Tone Predictor

Conventional Automatic Exposure Control

As mentioned earlier, exposure control plays a crucial role in adjusting the brightness of the photographed scene, while preserving its information content. The overall signal level in the captured and stored raw image data is determined by a set of controllable exposure parameters that are taking effect during the capture. Such exposure parameters [1-12] include the exposure time (the integration time), analog gain, digital gain, neutral density filter reduction factor, and stopped-down aperture reduction factor.

Let E_{total} denote the total effective exposure that results from the combination of all of the exposure parameters taking effect during the capture. A basic approach to determine the required total exposure, E_{total}, is to use a fixed target convergence level [1]. Let $M_{current}$ denote the average signal level calculated from the pre-processed raw camera data; the pre-processing includes at least linearization. Also let $E_{total,current}$ denote the total exposure that corresponds to $M_{current}$. The new total exposure $E_{total,new}$ is then calculated in such a way that the average signal level reaches a certain pre-determined target brightness level, M_{target}. $E_{total,new}$ is calculated as follows

$$E_{total,new} = E_{total,current} \times (M_{target} / M_{current}) \quad (4)$$

Figure 6 illustrates this basic approach for automatic exposure control. The parameters $M_{current}$ and M_{target} are overlaid on the hypothetical histograms of the pre-processed raw camera data. In practice, the convergence of the exposure takes place over multiple iterations, to account for the different non-linearities, such as pixel saturation, quantization to zero, remaining non-linearity in the dynamic range of the data, and temporally-varying illumination, which could otherwise cause oscillations in the exposure [1]. Many AEC algorithms are based on this same approach in one way or another [1, 5-8]. In most cases, the main differences include how different image areas are weighted in the calculation of the value that should converge to a given fixed target level, how exposure adjustment starting from an over-exposed condition is addressed, and how high-dynamic range scenes are tackled.

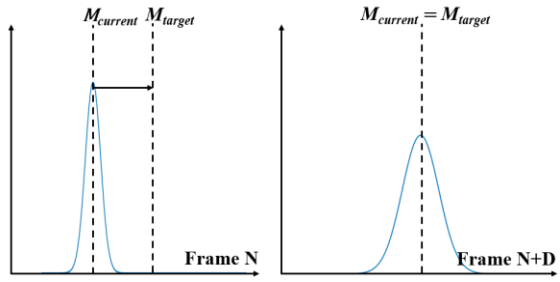

Figure 6 Illustration of the Convergence Target of a Conventional AEC Algorithm

Face Skin Tone Adaptive Brightness Targets

In the context of face-priority AEC, for proper exposure of faces of different skin tones, dark and bright ones, the face target brightness is adapted to the face skin tone, in order to avoid the face underexposure or overexposure. Figure 7 illustrates the proposed adaptation. The illustration is based on the bright face skin tone likelihood, L_{bright}. Since the sum of both of the dark and bright likelihoods is unity, one of them could be used in the mapping from the face skin tone likelihoods to the target brightness ranges. Referring to Figure 7, $B_{bright,min}$ and $B_{bright,max}$ denote the lower and upper bounds, respectively, on the target brightness for the bright face; and $B_{dark,min}$ and $B_{dark,max}$ denote the lower and upper bounds, respectively, on the target brightness for the dark face.

Let $B_{face,min}$ and $B_{face,max}$ denote the lower and upper bounds, respectively, on the target face brightness. The goal of the proposed face-priority exposure control is to adjust the target face brightness M_{target} such that $M_{target} \in [B_{face,min}, B_{face,max}]$. When L_{bright} is high (i.e. high confidence on the bright skin tone), $B_{face,max} = B_{bright,max}$ and $B_{face,min} = B_{bright,min}$. When L_{bright} is low (i.e. high confidence on the dark skin tone), $B_{face,max} = B_{dark,max}$ and $B_{face,min} = B_{dark,min}$. The lower and upper target brightness bounds linearly change in the transition

regions between the low-confidence regions (where the quality of the likelihood values is not high) and the high-confidence ones, as depicted in Figure 7, to avoid oscillations in the calculated target brightness and target exposure.

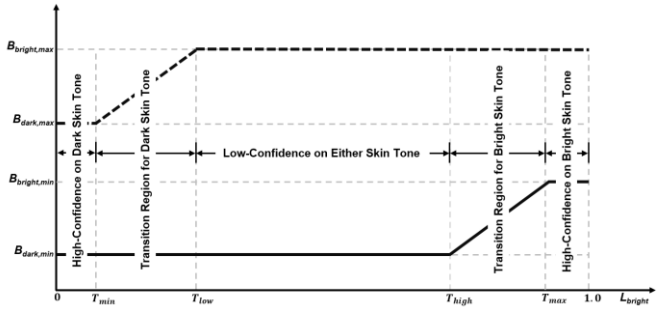

Figure 7 Adjustment of Brightness Targets Based on the Face Skin Tone Likelihood

When the quality of the face skin tone likelihoods is not high (low-confidence region), FaSTA AEC falls back to a conventional face-priority AEC; the lower and upper bounds on the face target brightness are set to $B_{face,min} = B_{dark,min}$ and $B_{face,max} = B_{bright,max}$, respectively. The target brightness bounds are *tunable*, and are selected to meet end-user preferences. The likelihood thresholds T_{min}, T_{low}, T_{high} and T_{max}, which mark the boundaries of the high-confidence, low-confidence and transition regions, are selected experimentally based on the FSTP performance.

Experimental Results

In this section, example results are presented and discussed for two typical challenging scenarios. The likelihood thresholds T_{min}, T_{low}, T_{high} and T_{max}, are set to 0.25, 0.3, 0.7 and 0.75, respectively. The target brightness bounds $B_{bright,min}$, $B_{bright,max}$, $B_{dark,min}$ and $B_{dark,max}$ are set to 0.2, 0.5, 0.125 and 0.3, respectively.

A. Bright Face Against a Bright Background

In this high-contrast scenario, conventional exposure control will typically adjust the exposure to too low value, causing the face to be under-exposed as depicted in Figure 8(a) for a mannequin with a bright face, moving back and forth in front of a window with strong backlight behind the window blinds. With FaSTA exposure control, the exposure time is adjusted, rendering a well-exposed face as shown in Figure 8(b). One should note that how bright or dark the face would be is *tunable* via the bright face target brightness bounds, allowing different trade-offs between background and foreground exposure.

With face-priority exposure control that disregards the face skin tone, the brightness target would have been adjusted to a value in the range of $[B_{face,min}, B_{face,max}] = [0.125, 0.5]$ and the face could have been under-exposed. With FaSTA exposure control, the target brightness lower and upper bounds are calculated based on the bright skin tone likelihood to be $B_{bright,min} = 0.2$ and $B_{bright,max} = 0.5$, respectively. And the face average luma value (brightness) is bounded by $B_{bright,min} = 0.2$ as shown in Figure 8(d), and as a result the face is exposed better.

It is worth noting that the FSTP had a stable, correct operation, as shown in Figure 8(c); the bright skin tone likelihoods were consistently high. Consequently, the calculated target brightness upper and lower bounds were stable, and there were no observed fluctuations in the scene brightness.

Figure 8(e) depicts the exposure time for conventional AEC, followed by FaSTA AEC. When face skin tone adaptation is enabled, there is a convergence period, where the exposure time gradually increases to meet the desired target brightness. That convergence period can also be seen in Figure 8(d), where the face average luma value increases gradually to meet the calculated target face brightness.

B. Dark Face Against a Dark Background

In this scenario, conventional exposure control will typically adjust the exposure to too high value, causing the face to be over-exposed as depicted in Figure 9(a) for a mannequin with a dark face, moving back and forth in front of a black background. In this test case, there is a side light, to introduce variation in the reflections on the face as it moves back and forth. With FaSTA exposure control, the exposure time is adjusted, rendering a well-exposed face as shown in Figure 9(b). How bright or dark the face would be is tunable via the dark face target brightness bounds.

With face-priority exposure control that disregards the face skin tone, the brightness target would have been adjusted to a value in the range of $[B_{face,min}, B_{face,max}] = [0.125, 0.5]$ and the face could have been over-exposed. With FaSTA exposure control, the target brightness lower and upper bounds are calculated based on the dark skin tone likelihood to be $B_{dark,min} = 0.125$ and $B_{dark,max} = 0.3$, respectively. And the face average luma value (brightness) is bounded by $B_{dark,min} = 0.125$ as shown in Figure 9(d), and as a result the face is exposed better.

Again, it is worth noting that the FSTP had a stable, correct operation, as shown in Figure 9(c); the dark skin tone likelihoods were consistently high. Consequently, the calculated target brightness upper and lower bounds were stable, and there were no observed fluctuations in the scene brightness.

Figure 9(e) depicts the exposure time for conventional AEC, followed by FaSTA AEC. When face skin tone adaptation is enabled, there is a convergence period, where the exposure time gradually decreases to meet the desired target brightness. That convergence period can also be seen in Figure 9(d), where the face average luma value decreases gradually to meet the calculated target face brightness.

Conclusions

In this paper, a novel face skin tone adaptive automatic exposure control solution was presented. This face-priority solution results in well-exposed faces in challenging capture scenarios. Experimental results demonstrated its superior performance over exposure control that does not take into account the face skin tone information. The solution is also easy to configure, and to tune to meet end-user preferences.

Future work includes extending the solution to tackle the following: 1) multiple faces of different sizes and skin tones in the scene; 2) non-frontal faces, where both of the eye positions may not be visible; 3) faces with occlusions, accessories, facial hair, strong facial expressions and various illumination changes, and 4) additional features, based on face skin color and intensity.

Acknowledgements

The authors would like to thank Jukka Kaartinen and John Mathew for their help with the experimental setup for testing the proposed solution.

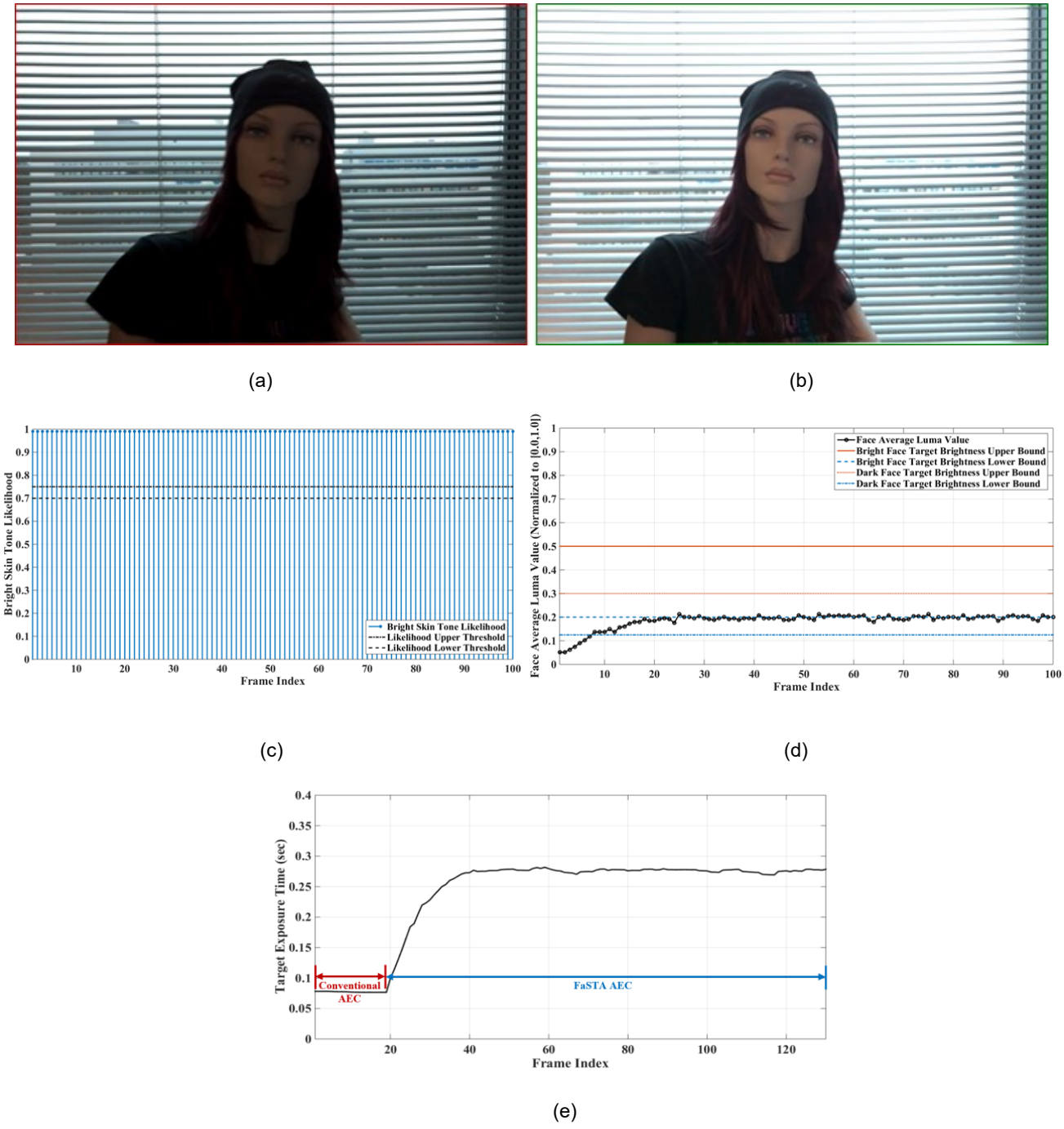

Figure 8 Results of Conventional and FaSTA AEC for a Bright Face Moving Against a Bright Background
(a) The conventional exposure control result for an example frame, (b) the FaSTA exposure control result for an example frame, (c) the bright skin tone likelihoods for 100 frames, (d) the face average, normalized luma value for the same 100 frames when FaSTA exposure control is enabled, (e) the target exposure time for conventional exposure control, followed by FaSTA exposure control

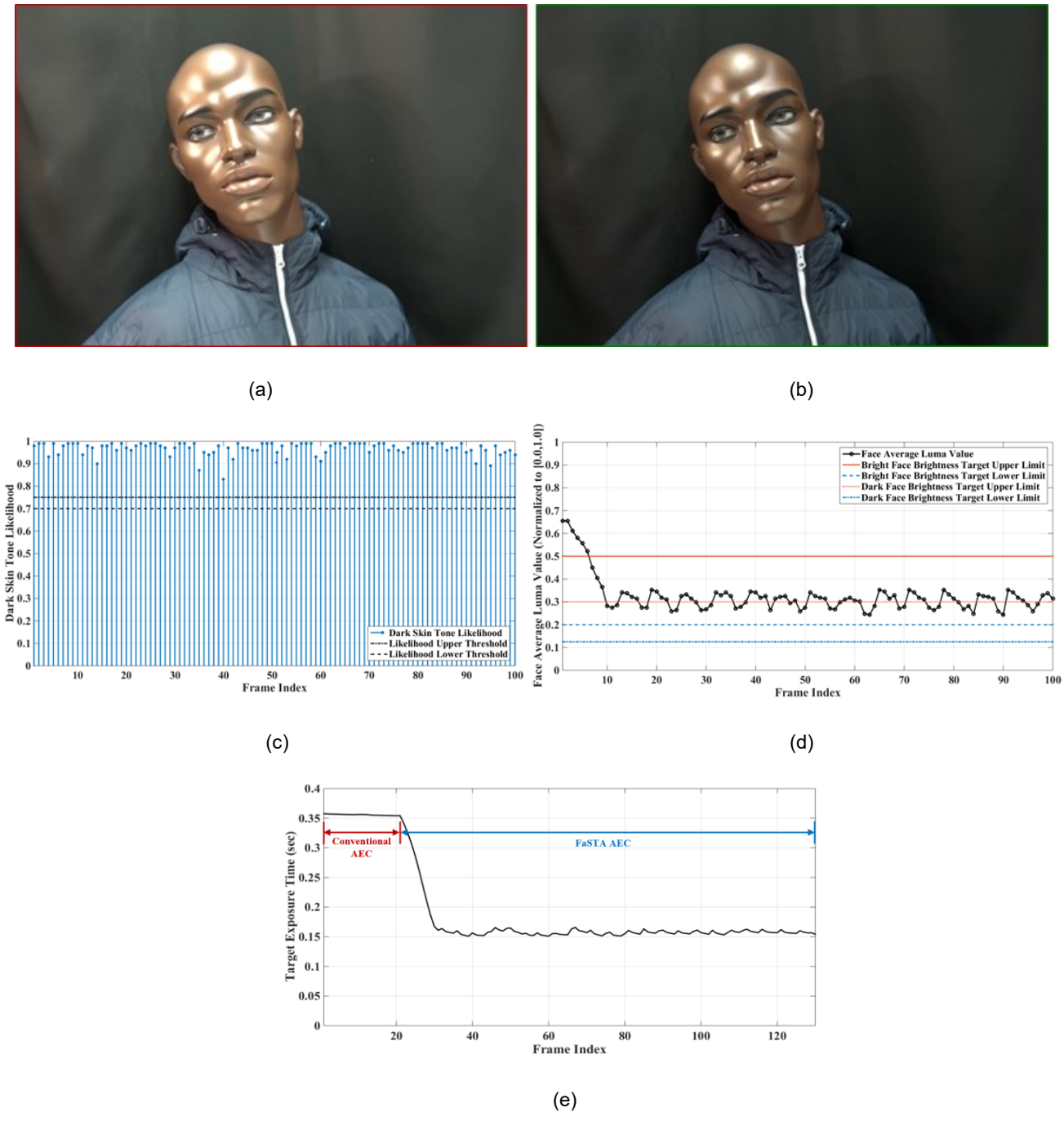

Figure 9 Results of Conventional and FaSTA AEC for a Dark Face Moving Against a Black Background
(a) The conventional exposure control result for an example frame, (b) the FaSTA exposure control result for an example frame, (c) the dark skin tone likelihoods for 100 frames, (d) the face average, normalized luma value for the same 100 frames when FaSTA exposure control is enabled, (e) the target exposure time for conventional exposure control, followed by FaSTA exposure control

References

[1] J. T. Nikkanen, "Computational Color Constancy in Mobile Imaging", ISBN 978-952-15-3074-6, 2013.

[2] J. T. Nikkanen and O. Kalevo, "Method and System in Digital Imaging for Adjusting Exposure and a Corresponding Device". US Patent 7 474 847, 2009 (priority date June 14th 2004).

[3] J. T. Nikkanen and O. Kalevo, "Method and system in digital imaging for adjusting exposure and a corresponding device". EP Patent 1652000 B1, 2009 (priority date, FI 20035113, June 30th 2003).

[4] J. T. Nikkanen and O. Kalevo, "Method and Apparatus for Adjusting Exposure in Digital Imaging". US Patent 8 013 909, 2011 (priority date December 29th 2004).

[5] T. Kuno, H. Sugiura and N. Matoba, "A new automatic exposure system for digital still cameras," IEEE Transactions on Consumer Electronics, vol. 44, no. 1, pp. 192-199, 1998.

[6] J.-S. Lee, Y.-Y. Jung, B.-S. Kim and S.-J. Ko, "An Advanced Video Camera System with Robust AF, AE, and AWB Control," IEEE Transactions on Consumer Electronics, vol. 47, no. 3, pp. 694-699, 2001.

[7] J. Liu, D. Ren, J. Zou, Y. Wu and S. Li, "Study of Automatic Exposure Algorithm Based on HD IP Camera," in International Conference on Advanced Intelligence and Awareness Internet (AIAI2010), Beijing, 2010.

[8] J. Liang, Y. Qin and Z. Hong, "An Auto-exposure Algorithm for Detecting High Contrast Lighting Conditions," in 7th International Conference on ASIC (ASICON2007), Guilin, 2007.

[9] H. Yang, Y. Chang, J. Wang and J. Huo, "A New Automatic Exposure Algorithm for Video Cameras Using Luminance Histogram," Frontiers of Optoelectronics in China, vol. 1, no. 3-4, pp. 285 - 291, 2008.

[10] S. Shimizu, T. Kondo, T. Kohashi, M. Tsuruta and T. Komuro, "A New Algorithm for Exposure Control Based on Fuzzy Logic for Video Cameras," IEEE Transactions on Consumer Electronics, vol. 38, no. 3, pp. 617 - 623, 1992.

[11] Q. K. Vuong, S.-H. Yun and S. Kim, "A New Robust Combined Method for Auto Exposure and Auto White-Balance," in Advances in Machine Learning and Data Analysis, Springer Netherlands, 2010, pp. 165 - 178.

[12] D. Ilstrup and R. Manduchi, "One-Shot Optimal Exposure Control," in ECCV'10 Proceedings of the 11th European conference on Computer vision: Part I, Heidelberg, Springer-Verlag Berlin, 2010, pp. 200 - 213.

[13] J. Nikkanen, P. Ahonen and T. Kaikumaa, "A method, system, and article provide automatic white balancing with skin tone correction for image processing". US patent US9398280 (priority date August 26, 2013)

[14] R. Hartley and A. Zisserman, "Multiple View Geometry in Computer Vision", Cambridge University Press, Second Edition, 2004.

[15] P. Viola and M. Jones, "Rapid object detection using a boosted cascade of simple features", Proceedings of the IEEE Conference on Computer Vision and Pattern Recognition (CVPR), 2001, pp. 511-518.

[16] H. Bay, T. Tuytelaars and L. V. Gool, "SURF: Speeded Up Robust Features", Proceedings of the 9th European Conference on Computer Vision, 2006, pp 404-417.

[17] V. Nair and G. E. Hinton, "Rectified linear units improve restricted boltzmann machines", Proceedings of the 27th international conference on machine learning (ICML-10). 2010. p. 807-814.

[18] A. L. Maas, A. Y. Hannun and A. Y. Ng, " Rectifier Nonlinearities Improve Neural Network Acoustic Models", Proceedings of the International Conference on Machine Learning, Vol. 30. No. 1. 2013.

[19] K. Ricanek Jr and T. Tesafaye, "MORPH: A Longitudinal Image Database of Normal Adult Age-Progression", IEEE 7th International Conference on Automatic Face and Gesture Recognition, 2006, pp 341-345.

[20] MORPH (Craniofacial Longitudinal Morphological Face Database): http://www.faceaginggroup.com/morph/

Authors Biography

Noha El-Yamany *received her B.Sc. and M.Sc. degrees in Electrical Engineering from Alexandria University in Alexandria, Egypt, in 1999 and 2002, respectively, and her Ph.D. degree in Electrical Engineering from Southern Methodist University in Dallas, Texas, USA, in 2010. Since 2012 she has been working at Intel Corporation in Tampere, Finland. Her focus areas include machine learning, camera algorithms, computational photography and real-time imaging architecture.*

Jarno Nikkanen *received his M.Sc. and Dr.Sc.Tech. degrees from Tampere University of Technology in 2001 and 2013, respectively, with subjects in Signal Processing and Software Systems. Jarno has 18 years of industry experience in digital imaging topics, starting at Nokia Corporation in 2000 where he developed and productized many digital camera algorithms, and moving to Intel Corporation in 2011 where he is currently working as Intel Principal Engineer and Imaging Technology Architect. Jarno holds international patents for over 20 digital camera related inventions.*

Jihyeon Yi *received her B.S. and M.S. degrees in Electrical Engineering from Korea Advanced Institute of Science and Technology, in 2005 and 2007, respectively. She has been working at Intel Corporation in Seoul, Korea since 2011. Her focus areas include facial attribute classification, face detection and face recognition.*

JOIN US AT THE NEXT EI!

IS&T International Symposium on

Electronic Imaging

SCIENCE AND TECHNOLOGY

Imaging across applications . . . Where industry and academia meet!

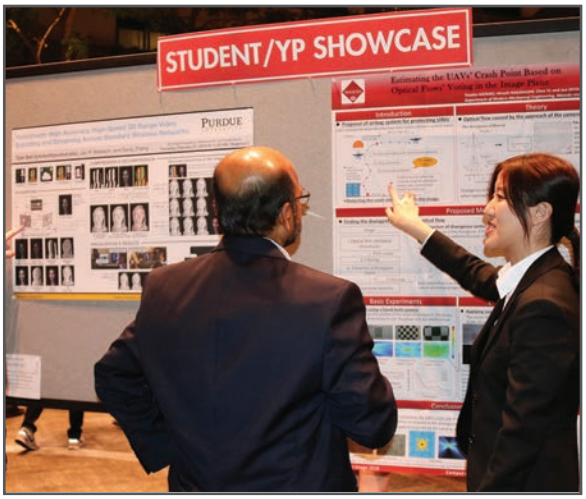

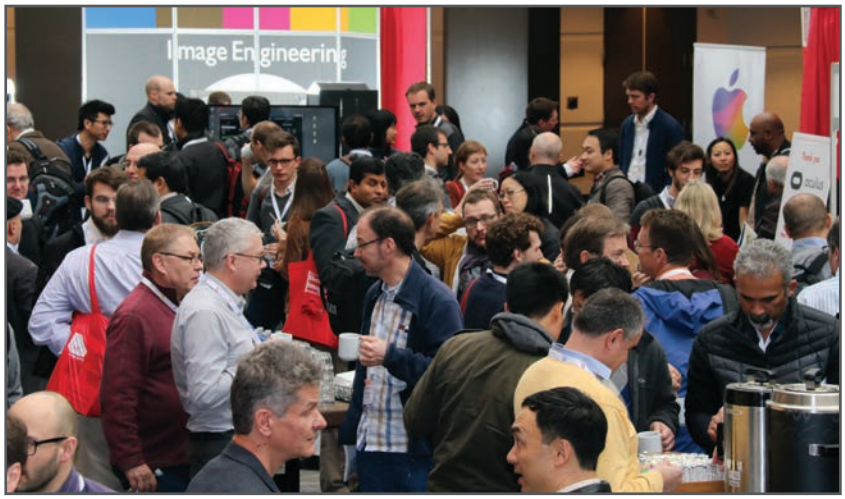

• SHORT COURSES • EXHIBITS • DEMONSTRATION SESSION • PLENARY TALKS •
• INTERACTIVE PAPER SESSION • SPECIAL EVENTS • TECHNICAL SESSIONS •

www.electronicimaging.org

IS&T
imaging.org